

# Correlation of Cone- and Rod-Derived Retinal Nonperfusion on Ultrawide Field Fluorescein Angiography with Diabetic Retinopathy Severity and Diabetic Macular Edema

Recivall P. Salongcay MD MPM<sup>1,2,3,4</sup>, Anna Karina D. Leopando MD<sup>1</sup>, Lizzie Anne C. Aquino BSc<sup>2</sup>, Tunde Peto MD PhD<sup>3</sup>, Paolo S. Silva MD<sup>1,2,5,6</sup>

<sup>1</sup>Eye and Vision Institute, The Medical City, Pasig, Metro Manila, Philippines

<sup>2</sup>Philippine Eye Research Institute, University of the Philippines, Manila, Philippines

<sup>3</sup>Centre for Public Health, Queen's University Belfast, Belfast, United Kingdom

<sup>4</sup>Department of Ophthalmology, Dr. Paulino J. Garcia Memorial Research and Medical Center, Cabanatuan City, Nueva Ecija, Philippines

<sup>5</sup>Beetham Eye Institute, Joslin Diabetes Center, Boston, Massachusetts, USA

<sup>6</sup>Department of Ophthalmology, Harvard Medical School, Boston, Massachusetts, USA

Correspondence: Recivall P. Salongcay

Office Address: Eye and Vision Institute, The Medical City, Pasig, Metro Manila, Philippines

Email Address: rpsalongcay@themedicalcity.com

Disclosure: Dr Salongcay has received conference travel support from Roche. Dr Leopando and Ms Aquino have no financial disclosures. Prof Peto has received financial support from Optomed and Optos, and is a consultant for Novartis, Bayer, Roche, Heidelberg and Optos. Dr Silva has received financial support from Optomed and Optos, and speaker's fees from Novartis, Bayer, Roche, Optos and Optomed.

## ABSTRACT

**Objective:** To evaluate cone- and rod-specific nonperfusion indices (CPI, RPI) on ultrawide field fluorescein angiography (UWF-FA) and their correlation with diabetic retinopathy (DR) severity and center-involving diabetic macular edema (ciDME).

### Methods

Sixty-nine eyes of 43 patients with diabetes underwent UWF color photography (UWF-CP), UWF-FA, and macular optical coherence tomography (OCT). DR severity was graded by a masked reader on UWF-CP. UWF-FA images were segmented into posterior pole ( $\leq 10$  mm from fovea), mid-periphery (10–15 mm) and far periphery ( $> 15$  mm), and into the macula, within ETDRS fields and extended peripheral fields. Ischemic areas were quantified using ImageJ to calculate nonperfusion index (NPI), CPI, and RPI. ciDME was determined on OCT. Correlations were analyzed using Pearson coefficients ( $r$ ).

### Results

DR severity correlated significantly with global NPI ( $r=0.56$ ,  $p<0.0001$ ) and across all retinal zones ( $r=0.35$ – $0.57$ ). Both CPI (global:  $r=0.56$ ,  $p<0.0001$ ; zones:  $r=0.42$ – $0.59$ ) and RPI (global:  $r=0.55$ ,  $p<0.0001$ ; zones:  $r=0.40$ – $0.59$ ) showed similar associations. ciDME presence was also correlated with NPI (global:  $r=0.40$ ,  $p=0.0014$ ; zones:  $r=0.42$ – $0.54$ ), CPI (global:  $r=0.47$ ,  $p=0.0001$ ; zones:  $r=0.32$ – $0.55$ ), and RPI (global:  $r=0.46$ ,  $p=0.0002$ ; zones:  $r=0.33$ – $0.54$ ).

### Conclusions

Cone- and rod-related retinal nonperfusion strongly correlate with DR severity and ciDME. UWF-FA may help identify high-risk eyes and guide surveillance of ischemia-related progression. Further studies are needed to define ischemic thresholds predictive of vision-threatening complications.

**Keywords:** diabetic retinopathy, diabetic macular edema, retinal ischemia, rods and cones, ultrawide field imaging

*Philipp J Ophthalmol* 2026;51:26-33



## INTRODUCTION

Diabetes mellitus (DM) is a major health concern, with prevalence projected to rise to 853 million by 2050.<sup>1</sup> Diabetic retinopathy (DR), the most common microvascular complication of DM, affects approximately 30-40% of individuals with Type 2 DM (T2DM) and up to 96% of those with Type 1 DM (T1DM) after 2 decades of disease.<sup>2, 3</sup> Poor glycemic control markedly increases the risk of DR, which remains the leading cause of vision impairment among working-age adults and a major cause of preventable blindness worldwide.<sup>4</sup> In the Philippines, an estimated 4.5 million adults or around 7.5% of the adult population were living with DM in 2024, underscoring the urgency of addressing DR.<sup>4, 5</sup>

Retinal ischemia is central to DR pathophysiology. Progressive capillary closure leads to alterations in perfusion status, hypoxia, and eventually vascular and neuronal dysfunction.<sup>6, 7</sup> Diabetic macular edema (DME), another vision-threatening complication, develops from the breakdown of the blood-retinal barrier due to chronic hyperglycemia, leading to macular thickening from fluid accumulation.<sup>7, 8</sup> Traditionally, DR severity is assessed using ETDRS standard 7-field fundus photographs, while DME is evaluated using stereoscopic photographs of the central 30° of the fundus (standard field 2).<sup>9</sup> Over recent decades, retinal imaging modalities have advanced considerably. Ultrawide field (UWF) imaging now permits visualization of the retinal far periphery, enabling more comprehensive evaluation of retinal pathology, while macular optical coherence tomography (OCT) has become the gold standard for detecting and monitoring DME due to its ability to delineate retinal layer microstructure.<sup>10, 11</sup> UWF fluorescein angiography (UWF-FA) further enhances DR assessment by quantifying nonperfusion areas, microaneurysm leakage, and neovascularization across the posterior pole and peripheral retina.<sup>8, 12-16</sup>

Evidence suggests that increasing retinal nonperfusion correlates with more advanced stages of DR; however, most prior studies predominantly focused on global retinal nonperfusion throughout all retinal zones without distinguishing regional or cell-specific contributions.<sup>8, 10, 11, 17</sup> Experimental

studies indicate that photoreceptors may play a pivotal role in diabetes-induced retinal capillary damage, with structural and functional alterations contributing to retinal ischemia.<sup>18</sup> These findings highlight the importance of evaluating the relationship between photoreceptor distribution, retinal nonperfusion, and DR progression.<sup>18</sup>

In this context, our study investigated whether segmentation of the retina into cone- and rod-rich regions, as well as topographic segments, reveals correlations between nonperfusion detected on UWF-FA, DR severity, and the presence of center-involving DME (ciDME). By exploring these associations, we aim to provide deeper insights into the pathophysiology of DR and its vision-threatening complications.

## METHODS

### *Population and Sample*

This is a single-site, cross-sectional, prospective study. Adult patients diagnosed with DM at The Medical City, Pasig, Metro Manila, Philippines were enrolled in the study. Inclusion criteria were as follows: (1) diagnosed case of T2DM; (2) 18 years of age or older; (3) presence of clear ocular media with adequate pupil dilation to obtain acceptable retinal imaging results; and (4) consented to undergo retinal imaging with pupil dilation. Exclusion criteria included (1) known allergy or hypersensitivity to fluorescein dye; (2) contraindication to pupil dilation; (3) history of prior panretinal photocoagulation (PRP) laser treatment; (4) presence of other retinal vascular disease aside from DR; (5) presence of dense cataracts or vitreous hemorrhage that prevents adequate view of the fundus; and (6) presence of any other ocular condition that prevents satisfactory completion of retinal imaging. The study protocol followed the tenets of 1964 Declaration of Helsinki and was approved by the Institutional Review Board of The Medical City. Informed consent was received from all study participants.

### *Image Acquisition and Analysis*

A total of 69 eyes from 43 patients diagnosed with T2DM underwent UWF color photos (UWF-CP) and UWF-FA using Optos California (Optos

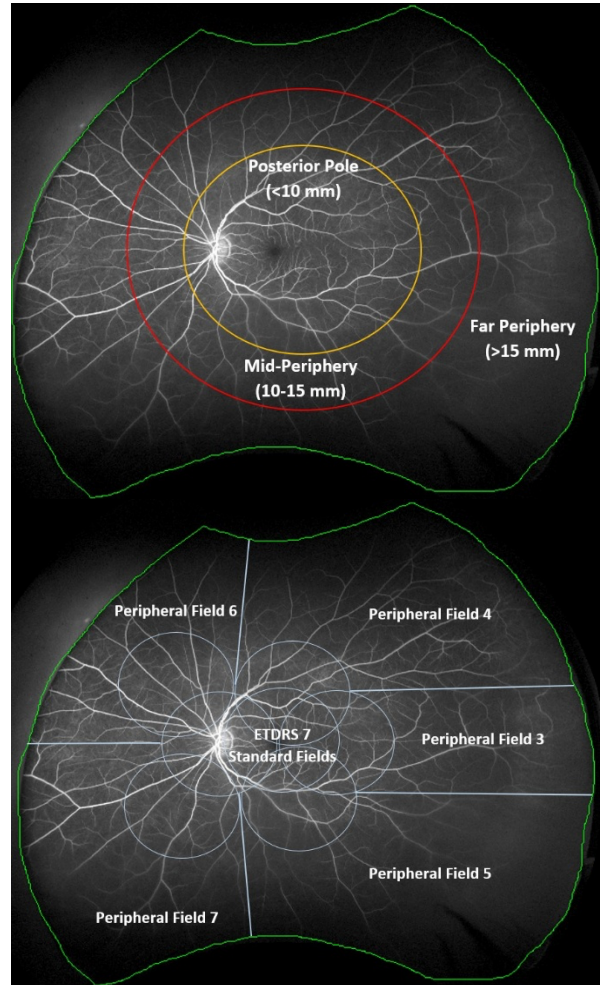
plc, Dunfermline, Scotland, UK) and macular OCT using Zeiss Cirrus 5000 (Carl Zeiss Meditec, Dublin, California, USA). Images acquired during the same visit were collected from the participants after pupil dilation with 1 drop of Tropicamide + Phenylephrine (0.5%/0.5%) eye drops. All images were de-identified and stored in a secure location.

The images were reviewed at a centralized reading center under controlled standardized conditions using high-definition, high-resolution LCD displays. DR was assessed on UWF-CP based on the International DR classification (i.e., no DR, mild nonproliferative DR [NPDR], moderate NPDR, severe NPDR and proliferative DR [PDR]), whereas the presence of ciDME (i.e., presence of retinal thickening, cystic changes or subretinal fluid at the macular central subfield) was evaluated using spectral domain OCT (SD-OCT) by a masked retina specialist proficient in UWF imaging and SD-OCT. A senior retina specialist conducted an independent secondary grading. In case of discrepancy, the final grade was determined through consensus agreement.

Using customizable software measurement tools provided by the imaging device supplier, UWF-FA images were segmented into different topographic zones: the posterior pole (within 10 mm from the foveal center), mid-periphery (10-15 mm) and far periphery (beyond 15 mm) as illustrated in Figure 1. The UWF images were projected stereographically and registered, and an ETDRS template and a peripheral fields template were digitally overlaid on the UWF image based on individual foveal and optic nerve head location. The digital overlay was used to further segment the image into (1) macula, (2) within ETDRS and (3) Peripheral Fields P3 to P7 as illustrated in Figure 2.

Ischemic areas were identified on UWF-FA using Image J (Fiji) software (National Institute of Health, Bethesda, Maryland USA) through a method described in detail in previous studies.<sup>6, 8, 19-22</sup> The total gradable area (TA) of each UWF-FA image was demarcated (in green) by drawing a free hand line using the Image J software (Figure 3) and saved as an image mask. Nonperfusion Areas (NPA) were identified and demarcated (in yellow) using the same method with the foveal avascular zone (FAZ) as reference for nonperfusion whenever possible. TA and NPA were calculated by adding the size of

all pixels that make up the mask while also correcting for peripheral distortion. The sums in pixels were converted into square mm. The Nonperfusion Index (NPI) was calculated within each retinal segment as NPA divided by TA. The software is also able to give a value for cone nonperfusion index (CPI) and rod nonperfusion index (RPI).



Figures 1 and 2. Topographic segmentation of UWF-FA images

Quantification of rods and cones in the UWF images was conducted by applying the technique described in previous studies by Croft et al and Sagong et al.<sup>23-25</sup> Concisely, histologic data on human photoreceptor topography<sup>26</sup> where the spatial density of both rods and cones assessed at increasing distances from the fovea (superiorly, inferiorly, nasally and temporally) was plotted onto a 3-dimensional model eye. Cell density maps can then be generated by interpolating these sampled

data points over the surface of the model eye (sphere) via inverse distance weighted averaging using MATLAB 2013a. This effectively estimates the photoreceptor density at any given location on the retina by measuring the distance (arc length) to the 8 nearest sampled histology points and applying a weighted average of their densities that reflects their respective distance to the location being interpolated. The density maps can then be accurately overlaid onto the UWF images using the Optos software, and with this both the surface area and density of cone and rod photoreceptors (cells/mm<sup>2</sup>) can be defined for every pixel; hence, the approximate number of rods and cones can be calculated for a selected area on the retina.

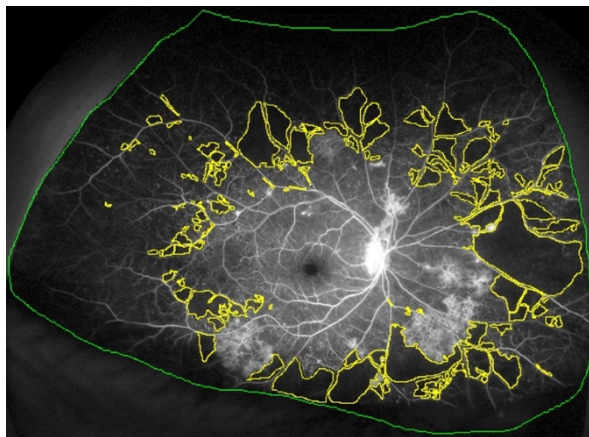


**Figure 3.** The total gradable area (TA) demarcated in green and nonperfusion area (NPA) demarcated in yellow using the FAZ as reference.

*Statistical Analysis*

The distribution of continuous variables was compared using Wilcoxon rank-sum test. Baseline demographic characteristics of participants were presented as means (standard deviation) or numeral values (percentage). The correlation between findings from UWF-CP, UWF-FA and SD-OCT was analyzed by using the Pearson correlation coefficient (r). Correlation was interpreted as follows: very weak correlation (interval of 0-0.199), weak correlation (0.20-0.399), moderate correlation (0.40-0.599), strong correlation (0.60-0.799), and very strong correlation (0.80-1.00). A p-value <0.05 was considered significant. Statistical analysis was performed using SAS ver. 9.4 (SAS Inc., Cary, NC, USA).

**RESULTS**

This study included 69 eyes from 43 patients with T2DM of 10.3 ± 7.7 years duration. Patients' baseline demographic characteristics are presented in Table 1. Image grading is summarized in Table 2. Out of the 69 eyes, 12 (17.4%) eyes were graded as having mild to moderate NPDR, 24 (34.8%) eyes with severe NPDR, and 21 (30.4%) eyes were graded with PDR. On SD-OCT, 15 out of 69 eyes (21.7%) presented with ciDME.

	Count ± SD or (n%)
Age, years	60.1 ± 9.5
Type 2 DM	67 (97.1)
DM duration, years	10.3 ± 7.7

	Count ± SD or (n%)
Diabetic Retinopathy Severity	
No DR	12 (17.4)
Mild to Moderate NPDR	12 (17.4)
Severe NPDR	24 (34.8)
PDR	21 (30.4)
Ungradable	0
ciDME	
Absent	54 (78.3)
Present	15 (21.7)

DM, diabetes mellitus; DR, diabetic retinopathy; NPDR, nonproliferative DR; PDR, proliferative DR; ciDME, center involving diabetic macular edema

Increasing DR severity on UWF color photos was correlated with increasing nonperfusion on UWF-FA. This remains significant even after distinguishing between cones and rods. The mean NPI, CPI and RPI of patients among the different severity levels of DR is presented in Figure 4. There is a linear trend when comparing nonperfusion of all three indices (NPI, CPI, RPI) with increasing DR severity. RPI was noted to be the highest at PDR stage. The trend suggests that increasing severity of DR is associated with worsening retinal ischemia.

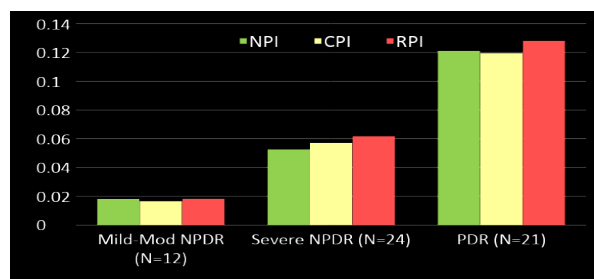


**Figure 4.** The correlation of diabetic retinopathy (DR) severity with nonperfusion index (NPI), cones nonperfusion index (CPI), and rods nonperfusion index (RPI).

**Table 3.** Correlation values of DR severity and presence of ciDME with NPI, CPI and RPI within each segmentation area of the fundus

	Entire Fundus	Posterior Pole	Mid-Periphery	Far Periphery	Macular	Within ETDRS	P3	P4	P5	P6	P7
<b>DR Severity</b>											
<b>NPI</b>	r=0.55944, p<0.0001	r=0.49902, p<0.0001	r=0.55251, p<0.0001	r=0.34536, p=0.006	r=0.40597, p=0.0011	r=0.50349, p<0.001	r=0.37752, p=0.0025	r=0.43884, p=0.0004	r=0.57411, p<0.0001	r=0.47896, p<0.0001	r=0.55364, p<0.0001
<b>CPI</b>	r=0.55617, p<0.0001	r=0.49231, p<0.0001	r=0.49231, p<0.0001	r=0.49231, p<0.0001	r=0.42368, p=0.0006	r=0.49783, p<0.0001	r=0.43379, p=0.0004	r=0.45817, p=0.0002	r=0.59082, p<0.0001	r=0.44896, p=0.0003	r=0.55273, p<0.0001
<b>RPI</b>	r=0.55285, p<0.0001	r=0.49268, p<0.0001	r=0.49268, p<0.0001	r=0.49268, p<0.0001	r=0.39798, p=0.0014	r=0.49339, p<0.0001	r=0.44759, p=0.003	r=0.45979, p=0.0002	r=0.59311, p<0.0001	r=0.43911, p<0.0004	r=0.55348, p<0.0001
<b>ciDME</b>											
<b>NPI</b>	r=0.39718, p=0.0014	r=0.53961, p<0.0001	r=0.27063, p=0.0334	r=0.06091, p=0.6381	r=0.51318, p<0.0001	r=0.53196, p<0.0001	r=0.24846, p=0.0515	r=0.25806, p=0.0429	r=0.28832, p=0.0231	r=0.44692, p=0.0003	r=0.42262, p=0.0006
<b>CPI</b>	r=0.46521, p=0.0001	r=0.55029, p<0.0001	r=0.55029, p<0.0001	r=0.55029, p<0.0001	r=0.51924, p<0.0001	r=0.54334, p<0.0001	r=0.32012, p=0.0112	r=0.32076, p=0.011	r=0.33106, p=0.0086	r=0.48529, p<0.0001	r=0.48359, p<0.0001
<b>RPI</b>	r=0.45586, p=0.0002	r=0.53882, p<0.0001	r=0.53882, p<0.0001	r=0.53882, p<0.0001	r=0.5082, p<0.0001	r=0.53388, p<0.0001	r=0.33211, p=0.0084	r=0.33034, p=0.0087	r=0.33557, p=0.0077	r=0.4813, p<0.0001	r=0.4944, p<0.0001
<span style="display: inline-block; width: 15px; height: 10px; background-color: #d9ead3; border: 1px solid black; margin-right: 5px;"></span> Moderate to strong correlation and statistically significant <span style="display: inline-block; width: 15px; height: 10px; background-color: #f4cccc; border: 1px solid black; margin-left: 20px; margin-right: 5px;"></span> Weak correlation and/or not statistically significant											

ciDME, center involving diabetic macular edema; NPI, nonperfusion index; CPI, cones nonperfusion index; RPI, rods nonperfusion index; UWF-FA, ultrawide field fluorescein angiography

There is a strong and statistically significant correlation with DR severity to NPI, CPI and RPI in the macula, within ETDRS and in all extended peripheral fields as shown above ( $r = 0.40-0.59$ ,  $p < 0.006$ ). This indicates that changes in DR severity are strongly related to the perfusion indices or changes in NPI, CPI and RPI across multiple areas of the retina. Both CPI and RPI also show a higher correlation with DR severity in P5 ( $r=0.59$ ,  $p<0.0001$ ).

Similarly, the presence of ciDME mostly shows a moderately strong correlation with nonperfusion. However, some areas (mid and far periphery, P3, P4 and P5) show weaker correlations or statistically non-significant compared to DR severity as shown by highlighted cells ( $r = 0.06-0.28$ ,  $p < 0.02 - 0.63$ ). This suggests that the relationship between ciDME and perfusion indices may be more localized and less prominent in the peripheral retina. In spite of that, the table shows a statistically significant correlation in most regions ( $r = 0.397-0.55$ ,  $p < 0.0001$ ), more significantly in the posterior pole ( $r = 0.55$ ,  $p < 0.0001$ ).

As the indices related to retinal nonperfusion (NPI, CPI, RPI) increase, there is a significant correlation with the severity of diabetic retinopathy. The findings are particularly strong for P5 ( $r = 0.57$ ,

$p < 0.0001$ ) and P7 ( $r = 0.55$ ,  $p<0.0001$ ). This indicates that all three indices show strong positive correlations with DR severity to a great degree in the far periphery. Within the macula, correlation values are slightly lower ( $r = 0.39$  to  $0.42$ ,  $p$ -value  $< 0.001$ ). Similarly, P3 presented with a slightly lower correlation ( $r = 0.377$ ,  $p < 0.003$ ) but is still considered moderately significant. In the ETDRS fields, correlations also remain moderate ( $r = 0.49$  to  $0.5$ ,  $p < 0.0001$ ) and also throughout P4 to P7 ( $r = 0.43$  to  $0.59$ ,  $p < 0.0001$ ). Thus, the values above show that in general there is a significant correlation with DR severity to NPI, CPI and RPI in the macula, within ETDRS and in all extended peripheral fields.

There is a strong and significant correlation with the presence of ciDME to NPI, CPI and RPI in the macula ( $r=0.5$ ,  $p<0.0001$ ), within ETDRS ( $r = 0.53$ ,  $p<0.0001$ ) and in extended peripheral fields 6 & 7( $r=0.44$ ,  $p<0.001$ ). They are however only weakly correlated in extended peripheral fields P3 ( $r = 0.24$ ,  $p < 0.0515$ ), P4 ( $r = 0.25$ ,  $p< 0.0429$ ) and P5 ( $r = 0.28$ ,  $p < 0.02$ ). The r-values are lower in general (0.23-0.33) while the p-values range from 0.007 to 0.05 which implies weaker correlation, though still statistically significant.

## DISCUSSION

The ETDRS established the first reproducible standard for grading retinal pathology, recommending 30° posterior pole photographs for quantification.<sup>9</sup> With the advent of UWF imaging, however, novel insights into retinal vascular disease have emerged. UWF imaging enables visualization of the peripheral retina, where nonperfusion is frequently more extensive, and allows quantification of retinal ischemia through ischemic index calculation to assess disease severity and predict complications.<sup>23, 27-29</sup>

Our single-site, cross-sectional, prospective study demonstrates that increasing DR severity on UWF-CP correlates with greater nonperfusion on UWF-FA. These findings are consistent with prior reports. Sedziak-Marcinek and colleagues observed retinal nonperfusion (RNP) in 4%, 51% and 49% of eyes with mild, moderate and severe NPDR, respectively.<sup>30</sup> Similarly, Ehlers et al. reported progressive increases in ischemic index – 0.095%, 1.37%, 2.80%, and 9.53% - from mild NPDR to PDR.<sup>31</sup> The DAVE and RECOVERY trials further established that DR progression is closely linked with the extent of both peripheral and posterior RNP.<sup>31</sup> Wykoff and colleagues emphasized that RNP is more frequently localized to the peripheral retina than the posterior pole, underscoring the importance of peripheral assessment in DR grading.<sup>31</sup>

Our study confirmed these associations across retinal subfields. DR severity correlated significantly with nonperfusion indices (NPI, CPI and RPI) in the macula, ETDRS fields, and all extended peripheral fields ( $r = 0.40-0.59$ ,  $p < 0.001$ ). The presence of ciDME also correlated with nonperfusion across these regions, with strongest associations in macular and nasal fields ( $r = 0.42-0.54$ ,  $p < 0.0005$ ). Conversely, weaker correlations were found in certain peripheral segments (P3-P5). These findings echo the DAVE study, which demonstrated disproportionate nonperfusion in the midperiphery compared to posterior and far-peripheral zones, and noted more leakage within posterior ischemic regions, possibly reflecting higher metabolic demand, giving rise to a higher predisposition to vascular leakage.<sup>31</sup>

The relationship between ischemia and DME is well established. Patel et al.<sup>28</sup> and Wessel et al.<sup>16</sup> reported that greater ischemic burden increases the likelihood of DME, with Wessel and colleagues noting a threefold higher risk in eyes with RNP. DME prevalence rises to as high as 71% in PDR. VEGF release from ischemic retina drives endothelial breakdown, vascular leakage, and edema, linking nonperfusion directly with macular complications.<sup>16, 32, 33</sup>

Beyond vascular changes, neuronal dysfunction is increasingly recognized in DR pathophysiology. Rods are utilized for dim-light/night vision or scotopic vision. Cones, on the other hand, are crucial for bright-light vision or photopic vision. The latter is also used for color discrimination and high visual acuity, particularly in the fovea.<sup>34</sup> Photoreceptors are highly metabolically active, and previous studies show early rod and cone impairment even before overt vascular pathology, likely driven by hyperglycemia, oxidative stress, and phototransduction-induced inflammation.<sup>35</sup> Our results suggest that photoreceptor dysfunction and rod involvement may progress alongside ischemia and DR severity, raising the possibility of rods serving as biomarkers for early disease progression. Understanding photoreceptor damage is vital in avoiding visual disturbance by improving early DR detection and more aggressive systemic management prior to occurrence of visual impairment.

Interestingly, parallels can be drawn from inherited retinal degenerations, where rod loss precedes cone dysfunction. Cones, however, often persist in a dormant state and remain capable of partial function.<sup>36</sup> This observation suggests that cones in DR may also represent therapeutic targets for interventions aimed at preserving daytime and high-acuity vision.

Overall, our study demonstrated proportional increases in NPI, CPI and RPI in DR severity, including in mild to moderate NPDR. These findings underscore the value of UWF-FA in identifying ischemia before advanced vision-threatening complications occur. Importantly, correlations between ciDME and nasal-field nonperfusion suggest that regional ischemia may carry distinct pathogenic relevance, warranting

further exploration of field-specific laser or targeted therapeutic strategies.

Our study has several strengths, including the use of UWF imaging analyzed at a centralized reading center with a standardized grading protocol, strict inclusion and exclusion criteria, and a prospective design. However, certain limitations should be acknowledged. The relatively small sample size may limit generalizability, and the manual grading of NPA and TA is labor-intensive and time-consuming. Future advances in automated software and image analysis could streamline this process, enhance reproducibility, and improve efficiency.

## CONCLUSION

Visual loss in DR arises primarily from DME and PDR, both usually late sequelae. However, our findings highlight that ischemia and photoreceptor dysfunction emerge much earlier. Identifying high-risk patients using UWF-derived ischemic indices may allow for earlier risk stratification and monitoring, intervention, optimized systemic management, and potentially novel neuroprotective or anti-ischemic therapies. Future work, including longitudinal studies, should aim to establish thresholds of ischemia predictive of vision loss, and clarify whether targeted treatment of ischemic subfields can alter disease trajectory.

## ACKNOWLEDGMENTS

The authors would like to thank Mr. Noel Cruz and Mr. Cloyd Pitoc for their assistance in the conduct of the study.

## FUNDING SOURCES

This study was funded in part by the UK Medical Research Council (MRC) and the Philippine Council for Health Research and Development (PCHRD) through the Newton-Agham Grant (Project Reference: MR/R025630/1). The funders had no role in the design or conduct of this study.

## ETHICS COMPLIANCE STATEMENT

The study protocol was reviewed and approved by the Institutional Review Board (IRB) of The Medical City (Ortigas Ave., Pasig City, Metro Manila, Philippines). Written informed consent was received from all study participants.

## REFERENCES:

1. IDF Diabetes Atlas, 11th ed. [database online]. Brussels, Belgium: International Diabetes Federation; 2025. <https://diabetesatlas.org/resources/idf-diabetes-atlas-2025/>.
2. Burton MJ, Ramke J, Marques AP, et al. The Lancet Global Health Commission on Global Eye Health: vision beyond 2020. *The Lancet Global health* 2021;9(4): e489–e551.
3. Bourne RR, Stevens GA, White RA, et al. Causes of vision loss worldwide, 1990-2010: a systematic analysis. *The Lancet Global health* 2013;1(6): e339–349.
4. The Lancet Diabetes E. Under the lens: diabetic retinopathy. *The lancet Diabetes & endocrinology* 2020;8(11): 869.
5. The Philippines [database online]. Brussels, Belgium: International Diabetes Federation; 2024. <https://idf.org/our-network/regions-and-members/western-pacific/members/the-philippines/>. Updated 2024.
6. Vujosevic S, Fantaguzzi F, Silva PS, et al. Macula vs periphery in diabetic retinopathy: OCT-angiography and ultrawide field fluorescein angiography imaging of retinal non perfusion. *Eye* 2024;38(9): 1668–1673.
7. Antonetti DA, Silva PS, Stitt AW. Current understanding of the molecular and cellular pathology of diabetic retinopathy. *Nature reviews Endocrinology* 2021;17(4): 195–206.
8. Silva PS, Dela Cruz AJ, Ledesma MG, et al. Diabetic Retinopathy Severity and Peripheral Lesions Are Associated with Nonperfusion on Ultrawide Field Angiography. *Ophthalmology* 2015;122(12): 2465–2472.
9. Grading diabetic retinopathy from stereoscopic color fundus photographs—an extension of the modified Airlie House classification. ETDRS report number 10. Early Treatment Diabetic Retinopathy Study Research Group. *Ophthalmology* 1991;98(5 Suppl): 786–806.
10. Cicinelli MV, Cavalleri M, Brambati M, et al. New imaging systems in diabetic retinopathy. *Acta diabetologica* 2019;56(9): 981–994.
11. Aiello LP, Odia I, Glassman AR, et al. Comparison of Early Treatment Diabetic Retinopathy Study Standard 7-Field Imaging With Ultrawide-Field Imaging for Determining Severity of Diabetic Retinopathy. *JAMA ophthalmology* 2019;137(1): 65–73.
12. Reddy S, Hu A, Schwartz SD. Ultra Wide Field Fluorescein Angiography Guided Targeted Retinal

- Photocoagulation (TRP). *Seminars in ophthalmology* 2009;24(1): 9–14.
13. Silva PS, Marcus DM, Liu D, et al. Association of Ultra-Widefield Fluorescein Angiography-Identified Retinal Nonperfusion and the Risk of Diabetic Retinopathy Worsening Over Time. *JAMA ophthalmology* 2022;140(10): 936–945.
  14. Sim DA, Keane PA, Rajendram R, et al. Patterns of peripheral retinal and central macula ischemia in diabetic retinopathy as evaluated by ultra-widefield fluorescein angiography. *American journal of ophthalmology* 2014;158(1): 144–153.e141.
  15. Oliver SC, Schwartz SD. Peripheral vessel leakage (PVL): a new angiographic finding in diabetic retinopathy identified with ultra wide-field fluorescein angiography. *Seminars in ophthalmology* 2010;25(1-2): 27–33.
  16. Wessel MM, Nair N, Aaker GD, et al. Peripheral retinal ischaemia, as evaluated by ultra-widefield fluorescein angiography, is associated with diabetic macular oedema. *The British journal of ophthalmology* 2012;96(5): 694–698.
  17. Jorgensen CM, Hardarson SH, Bek T. The oxygen saturation in retinal vessels from diabetic patients depends on the severity and type of vision-threatening retinopathy. *Acta ophthalmologica* 2014;92(1): 34–39.
  18. Kern TS, Berkowitz BA. Photoreceptors in diabetic retinopathy. *J Diabetes Invest* 2015;6(4): 371–380.
  19. Silva PS, Cavallerano JD, Sun JK, et al. Peripheral lesions identified by mydriatic ultrawide field imaging: distribution and potential impact on diabetic retinopathy severity. *Ophthalmology* 2013;120(12): 2587–2595.
  20. Fan W, Nittala MG, Velaga SB, et al. Distribution of Non-perfusion and Neovascularization on Ultra-Wide Field Fluorescein Angiography in Proliferative Diabetic Retinopathy (RECOVERY Study): Report 1. *American journal of ophthalmology* 2019.
  21. Fan W, Wang K, Ghasemi Falavarjani K, et al. Distribution of Nonperfusion Area on Ultra-widefield Fluorescein Angiography in Eyes With Diabetic Macular Edema: DAVE Study. *American journal of ophthalmology* 2017;180: 110–116.
  22. Salongcay RP, Aquino LAC, Salva CMG, et al. Comparison of Diabetic Retinopathy Lesions Identified Using Ultrawide Field Imaging and Optical Coherence Tomography Angiography. *Ophthalmic research* 2023;66(1): 1053–1062.
  23. Croft DE, Wykoff CC, van Hemert J, et al. Not All Retina Is Created Equal: Metabolic Quantification of Ultra-Widefield Images. *Ophthalmology* 2015;122(12): 2580–2582.
  24. Croft DE, van Hemert J, Wykoff CC, et al. Precise montaging and metric quantification of retinal surface area from ultra-widefield fundus photography and fluorescein angiography. *Ophthalmic Surg Lasers Imaging Retina* 2014;45(4): 312–317.
  25. Sagong M, van Hemert J, Olmos de Koo LC, et al. Assessment of accuracy and precision of quantification of ultra-widefield images. *Ophthalmology* 2015;122(4): 864–866.
  26. Curcio CA, Sloan KR, Kalina RE, et al. Human photoreceptor topography. *J Comp Neurol* 1990;292(4): 497–523.
  27. Spaide RF. Peripheral areas of nonperfusion in treated central retinal vein occlusion as imaged by wide-field fluorescein angiography. *Retina (Philadelphia, Pa)* 2011;31(5): 829–837.
  28. Patel RD, Messner LV, Teitelbaum B, et al. Characterization of Ischemic Index Using Ultra-widefield Fluorescein Angiography in Patients With Focal and Diffuse Recalcitrant Diabetic Macular Edema. *American journal of ophthalmology* 2013;155(6): 1038–1044.e1032.
  29. Tsui I, Kaines A, Havunjian MA, et al. Ischemic index and neovascularization in central retinal vein occlusion. *Retina (Philadelphia, Pa)* 2011;31(1): 105–110.
  30. Sędziak-Marcinek B, Teper S, Chelmecka E, et al. Diabetic Macular Edema Treatment with Bevacizumab Does Not Depend on the Retinal Nonperfusion Presence. *Journal of diabetes research* 2021;2021: 6620122.
  31. Wykoff CC, Yu HJ, Avery RL, et al. Retinal non-perfusion in diabetic retinopathy. *Eye (London, England)* 2022;36(2): 249–256.
  32. Lange J, Hadziahmetovic M, Zhang J, et al. Region-specific ischemia, neovascularization and macular oedema in treatment-naïve proliferative diabetic retinopathy. *Clinical & Experimental Ophthalmology* 2018;46(7): 757–766.
  33. Adamis AP, Miller JW, Bernal MT, et al. Increased vascular endothelial growth factor levels in the vitreous of eyes with proliferative diabetic retinopathy. *American journal of ophthalmology* 1994;118(4): 445–450.
  34. Functional Specialization of the Rod and Cone Systems. In: Purves D AG, Fitzpatrick D, Katz LC, LaMantia AS, McNamara JO, Williams SM, ed. *Neuroscience*. 2nd ed. Sunderland (MA): Sinauer Associates; 2001.
  35. Becker S, Carroll LS, Vinberg F. Diabetic photoreceptors: Mechanisms underlying changes in structure and function. *Vis Neurosci* 2020;37: E008.
  36. Ellis EM, Paniagua AE, Scalabrino ML, et al. Cones and cone pathways remain functional in advanced retinal degeneration. *Curr Biol* 2023;33(8): 1513–1522.e1514.